ELSEVIER

Journal of Power Sources 109 (2002) 230–233

JOURNAL OF POWER SOURCES

www.elsevier.com/locate/jpowsour

Short communication

Nano-scale Cu_6Sn_5 anodes

J. Wolfenstine*, S. Campos, D. Foster, J. Read, W.K. Behl

Army Research Laboratory, AMSRL-SE-DC, 2800 Powder Mill Road, Adelphi, MD 20783-1197, USA

Received 1 December 2001; accepted 15 January 2002

Abstract

Nano-scale (<100 nm) Cu_5Sn_6 powders were prepared by a chemical method that used a $NaBH_4$ solution to reduce the metal ions. A significant improvement in capacity retention was obtained in the nano-scale Cu_6Sn_5 alloy, compared to the alloy having micron-sized particles. The volumetric capacity of the nano-scale Cu_6Sn_5 alloy at 100 cycles was almost twice the theoretical capacity of graphite. Published by Elsevier Science B.V.

Keywords: Nano-scale; Li-ion; Batteries; Capacity; Anode

1. Introduction

In recent years, there has been a renewed interest in the use of metals such as Al, Bi, Sn, Si and Ge that alloy with Li as replacement anodes for graphite in Li-ion batteries [1–5]. Alloys offer significant advantages such as higher specific capacity and improved safety compared to graphite. However, there is one major problem that must be solved before they can be used in commercial and military applications. The major problem with alloys is the very large change in volume on charge and discharge which leads to stresses that cause the alloy to fracture and hence, disintegration of the anode. One potential solution to solve the fracture problem is to surround the alloy with an inert metal/ceramic/polymer matrix [1–14].

In this regard, work has been recently conducted on the Cu_6Sn_5 alloy in the Cu–Sn system to study its electrochemical reaction with Li and cycle life [15–18]. It has been shown as Li is inserted into Cu_6Sn_5 it first reacts to form $Li_2Cu_6Sn_5$, with further Li addition $Li_2Cu_6Sn_5$ decomposes into a Li–Sn alloy ($Li_{4.4}Sn$) surrounded by a Cu matrix [15–17]. The volumetric capacity of the Cu_6Sn_5 alloy made by melting Cu and Sn powders and then grinding and sieving the melted material to less than 38 μm was about twice that for graphite after 10 cycles when cycled between 0.0 and 1.2 V [16]. Another study prepared the Cu_6Sn_5 alloy by a variety of techniques: mechanical alloying, gas-atomization and melt-spinning [18]. Of the three techniques, the highest capacity retention after 60 cycles was observed in the mechanical alloyed material when cycled between 0.0 and 1.5 V. The volumetric capacity of the mechanical alloyed material was about three times that for the melted Cu_6Sn_5 alloy [16], after 25 cycles. It was suggested that one possible reason for the improved capacity retention was a result of the shorter-diffusion path in the mechanical alloyed material compared to the melted material. The mechanical alloyed Cu_6Sn_5 exhibited a flake morphology, with <1 μm thickness. Consequently, it is of interest to determine if a further improvement in capacity retention of the Cu_6Sn_5 alloy can be obtained when the particle size is reduced to the nano-scale range (<100 nm).

It is the purpose of this paper to investigate the capacity retention of the Cu_6Sn_5 alloy, when the particle size is reduced to the nano-scale (<100 nm) and compare it to that for the melted and mechanical alloyed Cu_6Sn_5 materials.

2. Experimental

Nano-scale Cu_6Sn_5 powders were synthesized by a chemical method, which involved reducing a methanol solution of $CuCl_2$ and $SnCl_2$ (1.2/1 volume ratio) with $NaBH_4$ in a 14 M NaOH solution under constant stirring at room temperature. Twice the amount of the $NaBH_4$ solution was added to the methanol solution containing the Cu and Sn ions to ensure complete reduction of the metal ions. Upon addition of the $NaBH_4$ solution a black precipitate was observed immediately. The black precipitate was washed with distilled water and filtered until the pH of the filtrate was the same as that of the distilled water. The precipitate was then dried at 100 °C under vacuum.

* Corresponding author. Tel.: +1-301-394-0317; fax: +1-301-394-0273.
E-mail address: jwolfenstine@arl.army.mil (J. Wolfenstine).

0378-7753/02/$ – see front matter. Published by Elsevier Science B.V.
PII: S0378-7753(02)00061-7

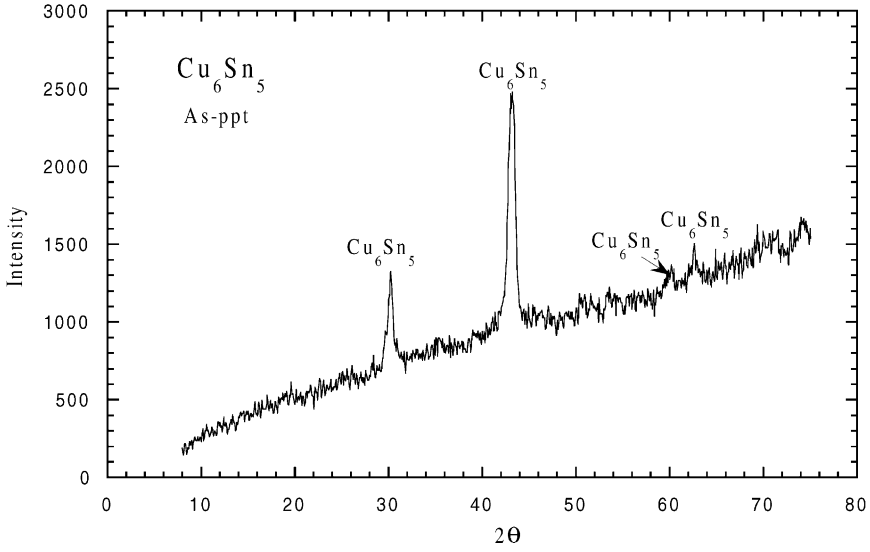

Fig. 1. X-ray diffraction pattern of the as-precipitated material.

The powders were characterized by X-ray diffraction, scanning electron microscopy (SEM) and transmission electron microscopy (TEM). Powders for TEM were prepared by dispersing them in methanol and while in an ultrasonic bath a drop of the suspension was placed on a Ni grid covered with an amorphous carbon film.

The cycle life of the Cu_6Sn_5 powders were evaluated in half-cells at room temperature. Cu_6Sn_5 positive electrodes were prepared by mixing 85 wt.% alloy powders, 5 wt.% carbon and 10 wt.% polyvinylidene fluoride dissolved in *N*-methylpyrrolidinone. The mixture was coated onto a Cu substrate. The electrodes were dried under vacuum. Metallic lithium was used as the negative electrode. The electrolyte solution was 1 M $LiPF_6$:ethlylene carbonate/dimethyl carbonate/diethyl carbonate (5/4/1 by volume). The cells were cycled at a constant current density of 0.1 mA/cm^2 between 0.0 and 1.0 V.

3. Results and discussion

Fig. 1 is an X-ray diffraction pattern of the Cu_6Sn_5 powders after precipitation. From Fig. 1, it can be observed that the precipitate was single-phase Cu_6Sn_5. No other Cu–Sn phases or pure component (Cu or Sn) peaks were exhibited in the X-ray diffraction pattern. The average crystallite size calculated using the Scherrrer formula [19] was 10 nm. X-ray microanalysis on particles that were cold-mounted and polished revealed the Cu and Sn were uniformly distributed with a Cu/Sn of about 1/1, which is in good agreement with the desired Cu/Sn of 1.2/1 for the Cu_6Sn_5 alloy. SEM analysis revealed the particles exhibited an equiaxed morphology with all particles less than 100 nm. The average particle size determined using the line intercept method [20] on more than 200 particles, was estimated to be about 40 nm. TEM confirmed that all particles were nano-scale (<100 nm). Fig. 2 is a TEM photomicrograph of some nano-scale Cu_6Sn_5 powders. It shows equiaxed particles with a size between 30 and 40 nm.

The voltage versus time profile for the first two cycles of the nano-scale Cu_6Sn_5 alloy are shown in Fig. 3. From Fig. 3, two important points are noted. Firstly, the discharge curve for the first cycle is longer than that for the second cycle. The extra length of the discharge curve for the first cycle compared to the second cycle is most likely associated with irreversible Li loss (i.e. Li_2O formation) as a result of the

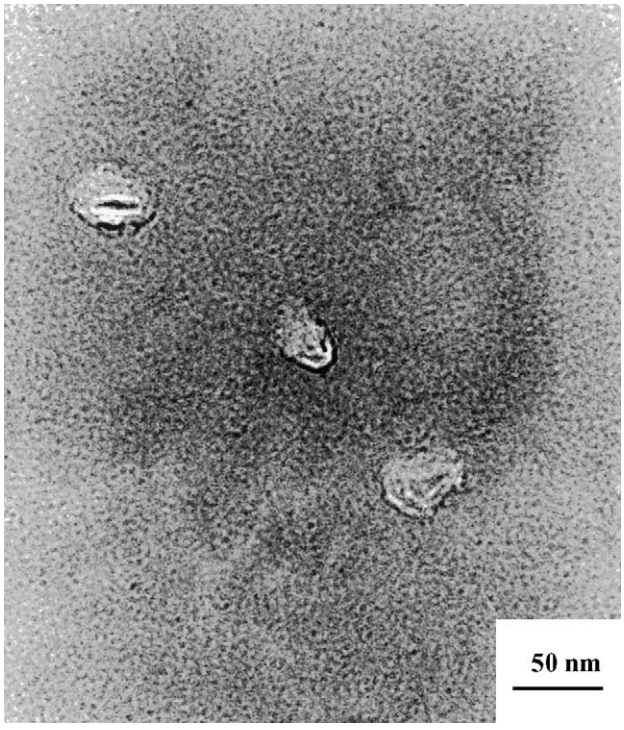

Fig. 2. Transmission electron photomicrograph of some nano-scale Cu_6Sn_5 powders.

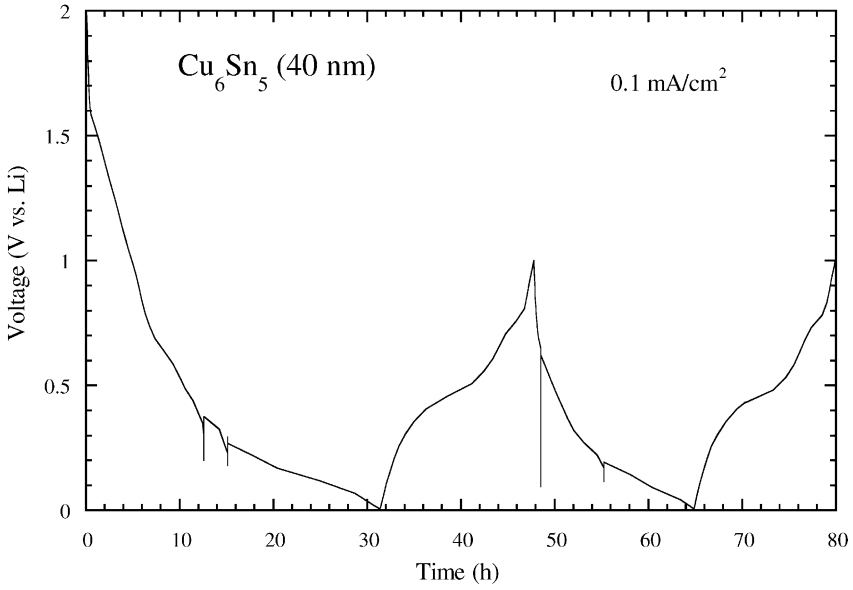

Fig. 3. The first and second cycle charge/discharge curves for the Li/Cu_6Sn_5 cell.

reduction of metal oxides (i.e. metal oxide → metal + Li_2O, upon initial Li titration) that are formed when the powders were handled in air during subsequent processing steps after precipitation and also from the reduction of the electrolyte solvent to form a solid electrolyte interphase on the particle surface. The second point is that the shape of the discharge curve is different from that observed for the micron-sized Cu_6Sn_5 powders that were prepared by melting, when discharged at a similar current density. From Fig. 3, it can be seen that there is a lack of well-defined plateaus in the second cycle discharge curve. In contrast micron-sized Cu_6Sn_5 powders, prepared by melting, exhibit a well-defined plateau around 0.4 V in the discharge curve [15–17]. A similar result has been observed in another metal-based composite system, where the effect of particle size on discharge performance was evaluated [21]. In Sn-based metallic composites it was found that as the particle size decreased, that well-defined plateaus observable in coarse powders (<45 μm) were impossible to distinguish in the finest powders (<0.2 μm) [20]. These results are in good agreement with the results for the Cu_6Sn_5 alloy, which also show that as the particle size is reduced, in this case to the nano-scale range, that well-defined plateaus observable in micron-sized powders disappear.

The volumetric capacity of the nano-scale Cu_6Sn_5 alloy (≈40 nm) versus cycle number is plotted in Fig. 4. Also shown in Fig. 4, is data for the melted (<38 μm) [16] and mechanical alloyed (<1 μm) [18] Cu_6Sn_5 materials. The current density for the melted and nano-scale materials was 0.1 mA/cm^2. It was 0.25 mA/cm^2 for the first five cycles, then 0.5 mA/cm^2 for the remaining cycles of the mechanical alloyed material. From Fig. 4, it can be observed that the extrapolated capacity approaches zero at about 45–50 cycles for the melted alloy and 80–85 cycles for the mechanical alloyed material. In contrast, at 100 cycles the nano-scale Cu_6Sn_5 powders still have a significant amount of

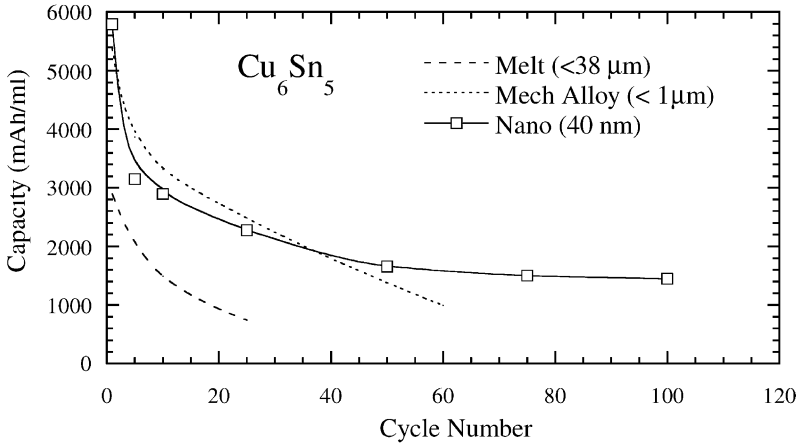

Fig. 4. Volumetric capacity versus cycle number for the nano-scale, melted [16] and mechanical alloyed [18] Cu_6Sn_5 materials cycled in the voltage range 0.0–1.0 V (nano-scale and melted) and 0.0–1.5 V (mechanical alloyed).

reversible capacity. This result shows that a large improvement in capacity retention of the Cu_6Sn_5 alloy is obtained when the particle size is reduced to the nano-scale range. The volumetric capacity of the nano-scale Cu_6Sn_5 alloy at 100 cycles (≈1450 mAh/ml) is almost twice the theoretical capacity of graphite (≈850 mAh/ml) [15].

4. Conclusions

The results of this study reveal that a significant improvement in capacity retention can be obtained when the particle size of the Cu_6Sn_5 alloy is reduced from the micron to the nano-scale range (<100 nm). The volumetric capacity of the nano-scale Cu_6Sn_5 alloy at 100 cycles is almost twice the theoretical capacity of graphite.

Acknowledgements

This work was performed under the Director's Research Initiative Program (FY01-SED-15) of the US Army Research Laboratory.

References

[1] M. Winter, J.O. Besenhard, Electrochim. Acta 45 (1999) 31.
[2] O. Crosnier, X. Devaux, T. Brousse, P. Fragnanaud, D.M. Schleich, J. Power Sources 97/98 (2001) 188.
[3] R.A. Huggins, J. Power Sources 81/82 (1999) 13.
[4] M. Winter, J.O. Besenhard, M.E. Spahr, P. Novak, Adv. Mater. 10 (1998) 725.
[5] J. Wolfenstine, J. Power Sources 79 (1999) 111.
[6] J. Yang, M. Wachtler, M. Winter, J. Besenhard, Electrochem. Solid State Lett. 2 (1999) 161.
[7] O. Mao, R.L. Turner, I.A. Courtney, B.D. Fredericksen, M.I. Buckett, L.J. Krause, J.R. Dahn, Electrochem. Solid State Lett. 2 (1999) 3.
[8] L. Fang, B.V.R. Chowdari, J. Power Sources 97/98 (2001) 181.
[9] O. Crosnier, T. Brousse, X. Devaux, P. Fragnanud, D.M. Schleich, J. Power Sources 94 (2001) 169.
[10] M. Maxfield, T.R. Jow, S. Gould, M.G. Sewchok, L.W. Shacklette, J. Electrochem. Soc. 135 (1988) 299.
[11] B.A. Boukamp, G.C. Lesh, R.A. Huggins, J. Electrochem. Soc. 128 (1981) 725.
[12] H. Li, X. Huang, L. Chen, Z. Wu, Y. Liang, Electrochem. Solid State Lett. 2 (1999) 547.
[13] G.X. Wang, L. Sun, D.H. Bradhurst, S. Zhong, S.X. Dou, H.K. Liu, J. Power Sources 88 (2000) 278.
[14] C. Wang, A.J. Appleby, F.E. Little, J. Power Sources 93 (2001) 174.
[15] K.D. Kepler, J.T. Vaughey, M.M. Thackeray, Electrochem. Solid State Lett. 2 (1999) 307.
[16] K.D. Kepler, J.T. Vaughey, M.M. Thackeray, J. Power Sources 81/82 (1999) 383.
[17] D. Larcher, L.Y. Beaulieu, D.D. MacNeil, J.R. Dahn, J. Electrochem. Soc. 147 (2000) 1658.
[18] Y. Xia, T. Sakai, T. Fujieda, M. Wada, H. Yoshinaga, J. Electrochem. Soc. 148 (2001) A471.
[19] B.D. Cullity, Elements of X-Ray Diffraction, Addison-Wesley, Reading, MA, 1978.
[21] M.I. Mendelson, J. Am. Ceram. Soc. 52 (1969) 443.
[20] J. Yang, Y. Takeda, N. Imanishi, O. Yamamoto, J. Electrochem. Soc. 146 (1999) 4009.